

THEORETICAL STUDIES ON THE ACYLATION REACTIONS OF AMMONIA BY KETENES: DETERMINATION OF REACTIVITY BY MOLECULAR ORBITAL THEORY (PART 54)

IKCHOON LEE AND CHANG HYUN SONG

Department of Chemistry, Inha University Incheon, 160 Korea

AND

TAE SEOP UHM

Department of Chemistry, Dong-A University Pusan, 600 Korea

ABSTRACT

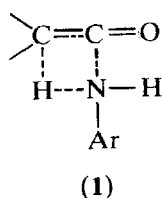
Theoretical studies on the reactions of ammonia with ketene and dimethylketene using the MNDO method are reported. The single step addition of ammonia to the olefinic bond of ketenes was found to provide a lower energy-barrier path than the two step carbonyl addition mechanism. The barrier height was lower in the reaction of ketene compared with that of dimethylketene in support of the faster rate of solution phase reactions of aniline and ketenes. The deformation energies of reactants had an overwhelming influence in determining the activation barriers in all the reactions investigated.

INTRODUCTION

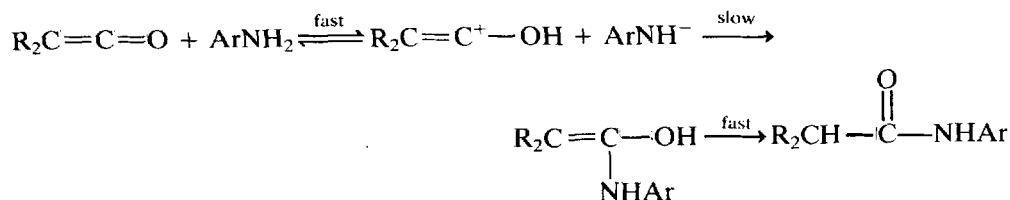
Acylation reactions of carboxylic acids, alcohols, and amines by ketenes have been widely studied owing to their industrial importance.¹ Blake and Davies² reported the gas phase kinetic studies on the addition of ketene to acetic acid to give acetic anhydride and proposed a six-center cyclic transition state (TS) formed by attachment of the carbonyl oxygen of the acid to the carbonyl carbon of ketene. On the other hand, Lillford and Satchell³ found for the reaction in ether of *m*-chloroaniline with ketene that the rate equation has the form given by equation (1).

$$\text{rate} = (k_1[\text{ArNH}_2] + k_2[\text{ArNH}_2]^2) [\text{ketene}] \quad (1)$$

This indicates the involvement of a path with one aniline molecule in the TS in addition to the dimer participation.⁴ They concluded that the reaction proceeds via a straightforward single step addition to the olefinic bond with the TS of structure (1).



In order to account for the low reactivity of dimethylketene relative to ketene, however, they considered the possibility of a carbonyl addition mechanism in which an ion-pair intermediate is formed prior to the rate determining attack on the α -carbon, as shown in Scheme 1.³



Scheme 1

Their HMO calculations on the atomic charge distributions indicated that the negative charge on the carbonyl oxygen of ketene is greater than that of dimethylketene, and the carbonyl oxygen has a greater negative charge than the β -carbon atom in both compounds (Table 1).

Table 1. Comparison of geometrical parameters and atomic charge distributions of ketene and dimethylketene^a ($R_1R_1C_2=C_3=O_4$)

	Method	Geometrical Parameters				Atomic Charges				Reference
		d ₁₂	d ₂₃	d ₃₄	L123	1	2	3	4	
Ketene	MNDO	1.085	1.319	1.184	121.78	+0.09	-0.28	+0.26	-0.17	This work
	<i>ab initio</i>					+0.22	-0.53	+0.24	-0.14	10
	HMO						-0.22	+0.49	-0.41	3
	Experim.	1.071	1.314	1.161	119.00					11
Dimethylketene	MNDO	1.503	1.330	1.181	120.56	+0.09	-0.35	+0.31	-0.16	This work
	HMO						-0.09	+0.47	-0.39	3

^ad in Å, angle in degree and charge in a.u.

In this work, in order to examine the mechanism of acylation reactions of amines by ketene, we have carried out the MNDO computations^{5a} on the reactions of ketene and dimethylketene with ammonia.

CALCULATIONS

The calculations were carried out using the standard MNDO procedure. Geometries of all species at stationary points on the potential energy surface were fully optimized using the

Davidon–Fletcher–Powell method.^{5b,c} Transition states were located by the reaction coordinate method,⁶ refined by the gradient norm minimization⁷ and characterized by confirming only one negative eigenvalue in the Hessian matrix.⁸ The TSs were also confirmed by the downhill energy optimization in both directions along the reaction coordinate to find the appropriate reactants, intermediates, and products.

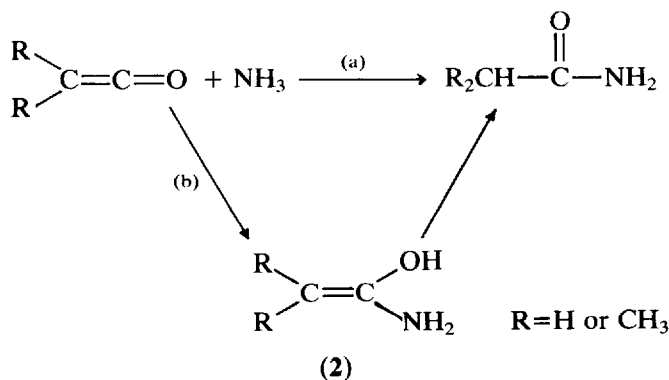
Zero-point energies, entropies, and enthalpy corrections for temperature changes were calculated using the procedures implemented in the AMPAC programs.⁹

RESULTS AND DISCUSSION

The optimized geometries and atomic charges of ketene and dimethylketene are compared with experimental and other MO results in Table 1. The MNDO geometries are seen to agree satisfactorily with those of the experimental values. Moreover our MNDO atomic charge distributions exhibit similar trends to those of the *ab initio* calculations. In contrast, the HMO atomic charges show a notable discrepancy as to the relative magnitude of negative charges on the carbonyl oxygen and the β -carbon atom. This is an important aspect with regard to the probable reaction path, since a greater negative charge on the carbonyl oxygen would favor the carbonyl addition mechanism in Scheme 1, whereas a greater negative charge on the β -carbon will favor the addition to the olefinic bond with the structure (1). In order to investigate the protonation behaviour of the ketenes, we have compared relative stabilities of the three protonated tautomers in Table 2. In excellent agreement with the *ab initio* values, our MNDO results predict the β -carbon protonation to be the most preferred form. It is therefore unlikely that an ion-pair is formed by protonating the carbonyl oxygen as in Scheme 1. In this work, we have disregarded the ion-pair intermediate and considered two paths : a single-step path, (a), and a two-step path, (b), which involves an intermediate (2) as shown in Scheme 2.

Table 2. Relative energies of protonated ketene tautomers (in kcal/mol)

	$\beta\text{-C-H}^+$	$\alpha\text{-C-H}^+$	O-H^+
MNDO	0	56.2	26.7
<i>ab initio</i> ¹¹	0	58.2	29.2



Scheme 2

Reaction Path ^b	ΔH_f^0	Reactant			S°	ΔH_f	TS1			Interm (2)	TS2	Prod.	ΔG^\ddagger
		Z_0	ΔH_f				Z_0	ΔH_f	S°				
K-a	-13.07	44.41	4.95	102.51	36.10	43.03	3.45	68.10			-47.99	56.53	
K-b	-13.07	44.41	4.95	102.51	35.72	43.63	3.11	65.42	-35.05	45.67	-47.99	57.21	
DK-a	-33.00	81.92	6.36	118.90	16.07	80.67	5.10	82.67			-54.88	57.36	
DK-b	-33.00	81.92	6.36	118.90	18.26	80.24	5.11	84.25	-49.73	25.03	-54.88	58.66	

Reference to Figures 1 and 2 also reveals that in all cases irrespective of the reaction path, ketene has a lower activation barrier ΔG^\ddagger than dimethylketene; this is again in agreement with the greater rate of reaction between ketene and *m*-chloroaniline found experimentally.³ It is also to be noted that the rate retardation with dimethylketene will be enhanced due to a greater steric repulsion, especially in the reactions with a bulky reactant, *m*-chloroaniline. This steric repulsion may also contribute to a facile olefinic addition, (3), compared with the sterically crowded carbonyl addition, (4).

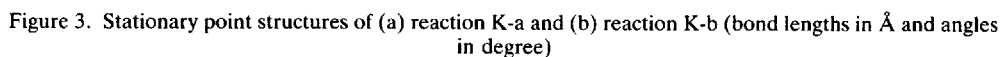
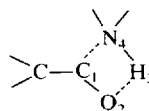
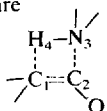


Table 4. Energy decomposition analysis for the reactions of ketenes and ammonia (kcal/mol)

Reaction Path ^a	D_f	I_n	$\Delta\Sigma 2\varepsilon_i$	$\Delta(V_{NN}-V_{cc})$
K-a	49.80	-0.62	-9.088	9.061
K-b	67.96	-19.16	-12.493	11.662
DK-a	58.34	-9.27	-5.289	4.887
DK-b	70.30	-19.04	-7.362	6.537

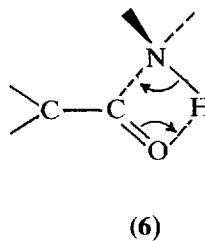
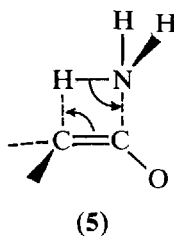
^aFor abbreviations, see text.Table 5. Variation of atomic charges in the reactions of ketenes and ammonia^a (a.u.)

Reaction Path ^b	Reactant				Deformed Fragment				TS ¹			
	1	2	3	4	1	2	3	4	1	2	3	4
K-a	-0.28	+0.26	-0.33	+0.08	-0.24	+0.24	-0.34	+0.14	-0.52	+0.41	-0.21	+0.24
K-b	+0.26	-0.17	+0.08	-0.23	+0.21	+0.20	-0.16	-0.38	+0.19	-0.44	+0.29	-0.18
DK-a	-0.35	+0.31	-0.23	+0.08	-0.32	+0.28	-0.36	+0.15	-0.56	+0.41	-0.22	+0.26
DK-b	+0.31	-0.61	+0.08	-0.23	+0.26	-0.19	+0.16	-0.38	+0.24	-0.43	+0.29	-0.19

^aNumbering schemes are for K-a and DK-a andfor K-b and DK-b.; ^bFor abbreviations, see text.

In this scheme A and B are the reactants, and A' and B' are the deformed fragments comprising the TS, A'—B'. The deformation and interaction energies are summarized in Table 4 for TS1 of the four reaction paths studied in this work. The interaction energies may be further subdivided into orbital energy changes, $\Delta\Sigma 2\varepsilon_i$, which reflect the effects of electron delocalization, non-bonded interactions etc.,¹⁷ and repulsive energy changes, $\Delta(V_{NN} - V_{cc})$, which can be taken to account for the net steric repulsion effect in the activation.¹⁸ The results in Table 4 clearly demonstrate the dominant influences, over 100%, of the deformation energy on the activation barrier, ΔH^\ddagger ; this is to be compared with ~70% contribution of D_f in the reaction of HCNO and H₂O¹⁹ and ~20% in the reaction of CH₂=C=NH with H₂O.²⁰

Atomic charges are summarized in Table 5 for reactants, deformed fragments and TS1. Notable charge variations occurring in the formation of deformed fragments are the increases in negative charge on N and positive charge on the transferring H. This corresponds to an incipient electron shift involved in a partial scission of the N—H bond. On the other hand, the changes in atomic charges accompanied in the TS formation from the two fragments (i.e., the negative charge decrease on N, the positive charge increases on transferring H and α -carbon, and the negative charge increase on β -carbon) indicate that the lone pair on N is mobilized in the formation of a partial bond between N and α -carbon and the olefinic π bond begins to break transferring part of π electrons toward β -carbon (or carbonyl oxygen in path (b)). The electron shifts involved in the activation follow the exact patterns that are expected in the product formation as shown in (5) and (6).



We conclude that the reactions of ammonia with ketenes take place through a single step addition to the olefinic bond, and the reactions are largely controlled by the deformation of reactants in the activation.

ACKNOWLEDGEMENTS

We thank the Ministry of Education and the Korea Science and Engineering Foundation for support of this work.

REFERENCES

1. P. G. Blake and M. H. B. Vayjooee, *J. Chem. Soc. Perkin 2*, **13**, 1533–1536 (1976).
2. P. G. Blake and H. H. Davies, *J. Chem. Soc. B*, 1727–1728 (1971).
3. P. J. Lillford and D. P. N. Satchell, *J. Chem. Soc. B*, 1016–1019 (1970).
4. (a) P. J. Lillford and D. P. N. Satchell, *J. Chem. Soc. B*, 889 (1968); (b) D. P. N. Satchell and R. S. Satchell, *Chem. Soc. Rev.*, **4**, 231–250 (1975).
5. (a) M. J. S. Dewar and W. Thiel, *J. Am. Chem. Soc.*, **99**, 4899–4907 (1977); (b) W. C. Davidon, *Comput. J.*, **1**, 406 (1968); (c) R. Fletcher and M. J. D. Powell, *Comput. J.*, **6**, 163 (1973).
6. (a) M. J. S. Dewar, *et al.*, **93**, 4290 (1971); (b) K. Muller, *Angew. Chem.*, **19**, 1 (1980).
7. (a) A. Komornicki, K. Ishida, and K. Morokuma, *Chem. Phys. Lett.*, **45**, 595 (1977); (b) J. W. McIver, Jr. and A. Komornicki, *J. Am. Chem. Soc.*, **94**, 2625–2633 (1972).
8. I. G. Csizmadia, *Theory and Practice of MO Calculations on Organic Molecules*, Elsevier, Amsterdam, 1976, p. 239.
9. Available from Quantum Chemistry Program Exchange (QCPE) No. 506.
10. A. G. Hopkinson, *J. Chem. Soc. Perkin 2*, 795–797 (1973).
11. H. R. Johnson and M. W. P. Strandberg, *J. Chem. Phys.*, **20**, 687 (1952).
12. J. W. Moore and R. G. Pearson, *Kinetics and Mechanism*, 3rd ed., Wiley, New York, 1981, p 290.
13. M. T. Nguyen, M. Sana, G. Leroy, *Bull. Soc. Chim. Boly*, **90**, 681 (1981).
14. M. J. S. Dewar, E. G. Zoebisch, E. F. Healy, and J. J. P. Stewart, *J. Am. Chem. Soc.*, **107**, 3902–3909 (1985).
15. G. S. Hammond, *J. Am. Chem. Soc.*, **77**, 334 (1955).
16. (a) I. H. Williams, *et al.*, *J. Am. Chem. Soc.*, **105**, 31–40 (1983); (b) H. Yamataka, S. Nagase, T. Ando, and T. Hanatusa, *J. Am. Chem. Soc.*, **108**, 601–606 (1986).
17. (a) I. Lee, Y. G. Cheun, and K. Yang, *J. Comput. Chem.*, **3**, 565–570 (1982); (b) I. Lee, Y. G. Cheun, K. Yang, and W. K. Kim, *J. Korean Chem. Soc.*, **26**, 195–204 (1982); (c) I. Lee, B.-S. Lee, and K. Yang, *Bull. Korean Chem. Soc.*, **4**, 157–161 (1983).
18. (a) N. D. Epiotis, R. L. Yates, and F. Bernardi, *J. Am. Chem. Soc.*, **97**, 5961–5970 (1975); (b) I. Lee, K. Yang, B. S. Park and K. S. Lee, *Bull. Korean Chem. Soc.*, **7**, 231–235 (1986).
19. M. T. Nguyen, *et al.*, *J. Am. Chem. Soc.*, **102**, 573–580 (1980).
20. M. T. Nguyen and A. F. Hegarty, *J. Am. Chem. Soc.*, **105**, 3811–3815 (1983).